Studying the behaviour of two chaotic systems

Clara Escanuela and Zhiyi Feng

10305726 and 10344201

University of Manchester

Department of physics and astronomy

April 2020

Abstract

Chaos was theoretically studied in two specific systems: the chaotic pendulum and the Belousov–Zhabotinsky reaction. We proved that these two cases of study exhibit the main properties of chaos: apparent stochastic behaviour and unpredictability. The presence of chaos was studied by applying nonlinear methods such as Lyapunov exponents, attractors, and bifurcation diagrams. Although we cannot claim to have shown that the systems are chaotic, the evidence that they are so is overwhelming.

1 Introduction

Chaos was first recognised by the meteorologist Edward Lorenz (1963) who widely studied the unpredictability of the weather. Chaotic systems behave irregularly and depend highly on initial conditions. Surprisingly, the apparently random behaviour of these systems seems to contradict their deterministic nature. "Certain systems may exhibit either periodic or irregular behaviour when there is no obviously related periodicity or irregularity in the forcing process" (Lorenz, 1963, p.140). One of the effects of the unpredictable behaviour of chaotic systems is the well-known "Butterfly effect" (Lorenz, 1972) that wonders whether or not the flap of a butterfly in Brazil can set off a tornado in Texas. The question may not be possibly answered but the unstability of the weather leads us to confirm the huge effect on the weather due to small changes in the atmosphere or initial conditions.

The mathematical theory of chaos is applied in many fields of study as it can be seen everywhere in nature. From physics to chemistry, here we computed a program to explore the chaotic behaviour of the driven damped nonlinear pendulum and use this to discover its implication to the Belousov–Zhabotinsky (BZ) chemical reaction. A simple pendulum can become a physical pendulum by adding dissipation, nonlinearity and a driving force. The damped driven pendulum, or chaotic pendulum, can display periodic and chaotic behaviours.

The BZ reaction was discovered by Belousov (1950) and analysed by Zhabotinsky (1961). It became important as the actual reaction mechanism is really

complex (it is still unknown) and far from thermodynamic equilibrium. Many models try to simplify the mechanism and explore the chaotic behaviour of the system. Here, we will examine one of them: the Gyögyi-field model.

The investigation on chaotic behaviours is one application of calculus (Acheson, 1997). Due to the development of computer science, many methods are available to solve ordinary differential equations, such as the Runge-Kutta method and the Bulirsch-Stoer method. In this project, we used the 4th order Runge-Kutta (RK4) method, which includes the Euler's method, to get numerical solutions of differential equations. The efficiency of the RK4 method ensures good results.

2 Concepts

The first logical step is to clarify and define the main and general concepts that are applying here.

We are specifically defining the chaos as "deterministic". Determinism and randomness will be used along with the report according to the concept of Randomization Kolmogorov-Chaitin. Data is produced randomly if the same string is its elegant program. A program refers to the instructions to generate a string of data, and the elegant program is the smallest possible one. Therefore, randomness occurs when the program that generates a string is as long as the string itself. As stated by Chaitin (2004, p.22), a random string is "one for which there is no program for calculating it that is substantially smaller than it is".

Furthermore, "chaos" is defined as the unpredictability due to the sensitivity to the initial conditions. Chaos has two main properties. First, the behaviour appears stochastic or irregular. The resulting pattern is its elegant program. Second, the future of the system is unpredictable because the system is extremely sensitive to initial conditions. A small change in initial conditions can be interpreted as an uncertainty in the measurements. This uncertainty leads to an error in the predictions that grows linearly for non-chaotic systems and exponentially for chaos. There are two necessary conditions for chaos: three independent dynamical variables and a nonlinear term in the differential equation that couples the variables (Baker and Gollub, 1996, pp.1-2).

The report aims to show that the properties of chaos are present in our cases of study. Chaos is not specifically shown, we can only prove that these systems follow the chaotic properties, which strongly suggests the presence of chaos.

3 Computational method

Throughout the work, we analytically solved the differential equations by using the fourth-order Runge-kutta method with python (Van Rossum and Drake, 1995). Firstly, we turned every higher order differential equation into coupled equations of first order. The solutions of the differential equations were found in the interval $[t_0, t]$ by dividing it into small steps of size h. The RK4 method calculates four points and their slopes between t_0 and $t_0 + h$ and the process is carried out over and over in a simple loop program until it reaches time t. The program gets the slope at time t_0 and uses that slope to step halfway through

the time step. Then it calculates the gradient at the midpoint ($t_0 + \frac{h}{2}$) and uses it to step halfway through the time step and calculate the slope at the midpoint between $t_0 + \frac{h}{2}$ and $t_0 + h$. Finally, the latter slope was used to step to $t_0 + h$ (Acheson, 1997, p.51). The error in the measurements is h^4 per step.

Before studying the chaotic pendulum, we checked the validity of our computing method by applying it to a simple pendulum under the small angle approximation. This simple system can be easily studied and the result of the equation of motion was manually calculated. The results were confirmed and the method was successfully tested.

We have alternated the RK4 method with a built-in function, the Scipy's "integrate.odeint" (Jones, et al. 2001), that made the code more efficient for plotting the bifurcation diagrams.

4 The chaotic pendulum

4.1 Models

The damped driven pendulum is usually referred to as the chaotic pendulum. This is a pendulum driven by an external force with amplitude f and on which a frictional force with damping term β acts. Therefore, the forces acting on the system are gravity (body force), the driving force, and the damping force. Newton's Second Law is used to write the dimensionless equation of motion of the driven damped pendulum:

$$\frac{d^2\theta}{dt^2} + \beta\frac{d\theta}{dt} + sin\theta = fcos(\Omega t), \tag{1}$$

where θ is the angle to the vertical, Ω is the driven angular frequency and t is the dimensionless time. Equation 1 can be transformed into coupled equations as follow,

$$\frac{d\omega}{dt} = -\beta\omega - sin\theta + fcos\phi, \tag{2}$$

$$\frac{d\theta}{dt} = \omega, \tag{3}$$

$$\frac{d\phi}{dt} = \Omega. \tag{4}$$

4.2 Simulations and results

4.2.1 Irregular behaviour

The first step is to calculate the dissipation of the system, which is the divergence of the velocity field (shown in equations 2 to 4). This gives a dissipation of -β. The value is negative; therefore, the system is dissipative and the volume of the phase space shrinks with time.

The behaviour of the pendulum is incredibly dependent on the parameters. Irregularity and periodicity are alternated with f. We studied the trajectory of the pendulum while keeping $\Omega = 2/3$ and $\beta = 0.5$ fixed and varying f. Two of the trajectories ($\theta - t$ graphs) can be seen in figures 1 and 2. The initial conditions were chosen to be 0.5 for ω and 0 for θ and ϕ.

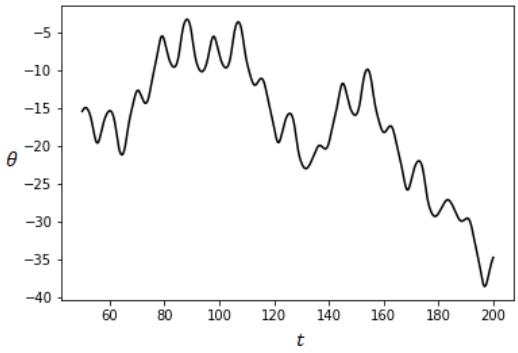

Figure 1: This graph represents θ against time, i.e. the trajectory of the pendulum when $f = 1.5$

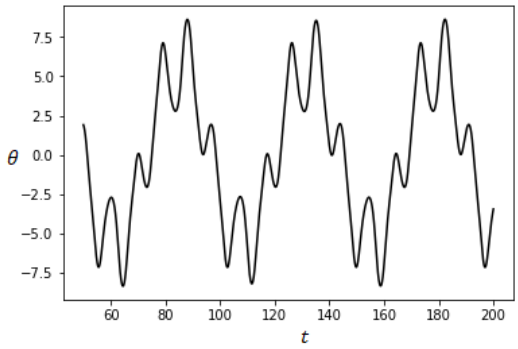

Figure 2: The trajectory of the pendulum for $f = 1.52$

Figure 2 represents regular motion in contrast with Figure 1 that exhibits a non-repeating motion, which is an example of chaotic behaviour. A small change in f, from 1.5 to 1.52, represents a significant change in the trajectories, from irregular to periodic motion.

We also evaluated the phase space. For simplicity, the phase space is plotting in two dimensions, omega against theta (needed variables to describe the state of the system). The third dimension (ϕ) is linearly related to time ($\propto \Omega t$) and is not considered. The angle θ is restricted between $-\pi$ and π.

The phase space of Figure 3 tells us when there are librations, rotations or an irregular alternation of both motions. The latter occurs when the motion is chaotically described.

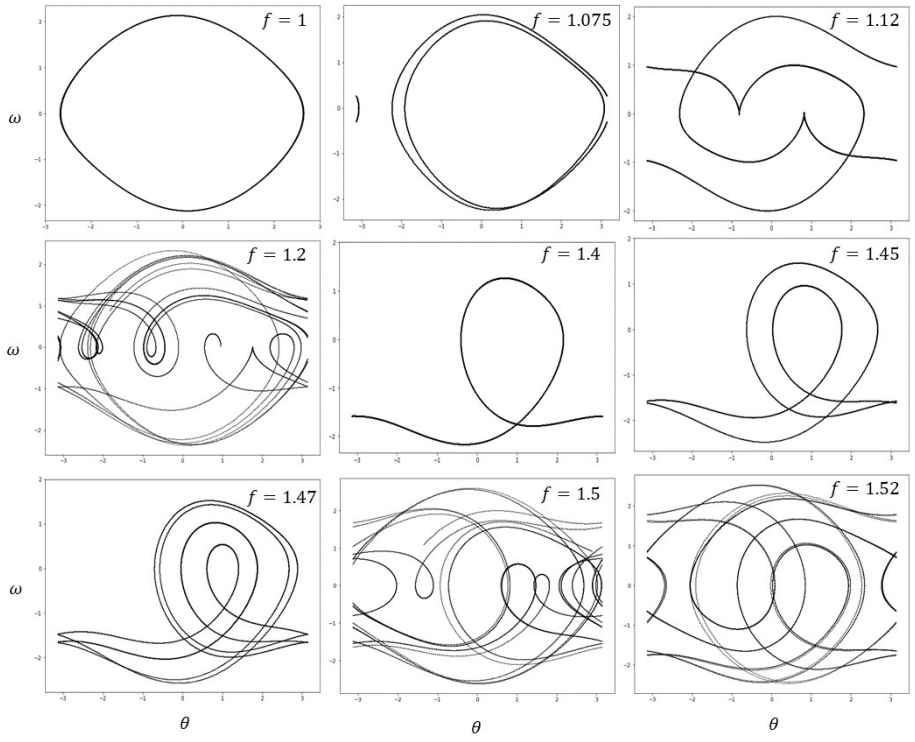

Figure 3: The phase space for different values of f

The behaviour of this dynamical system is influenced by the value of f. The nature of the solutions and/or the number of solutions change when passing a critical value of the parameter. At $f = 1$, the phase space is almost perfectly sinusoidal but somewhat distorted. When we change the value slightly (to $f = 1.075$) we see a period-doubling bifurcation that we will explain clearer later. At $f = 1.12$ we can see libration with angular frequency $\Omega/3$. Chaotic behaviour appears when $f = 1.2$ and $f = 1.5$, as there is no pattern associated with these phase graphs. For $f = 1.4$, 1.45 and 1.47, we find rotating solutions with periodic, doubling periodic, and second doubling periodic solutions. At $f = 1.52$, the solution exhibits periodic librations with period 5 (Greiner, 2009, p.539). This is represented in the bifurcation diagram, Figure 8. The graphs exhibit regular behaviours except when f is equal to 1.2 and 1.5.

Period doubling can be further explained with Figure 4 that represents the graph of θ against time with θ restricted from $-\pi$ to π. The values of f are 1.4 (left) and 1.45 (right). These are, as before, rotating solutions with a varying period. The graphs show sharp bumps and smaller bumps between them. The sharpest ones represent the period of the driving force. From smaller to higher f we can see that the number of different maxima increases. In the graph on the right, the period is doubled as the bumps, others than the sharpest ones, have two possible maxima and the graph on the left represents simply periodic rotating solutions as there is only one maximum. For $f = 1.47$, we will find four different maxima apart from the sharpest bumps.

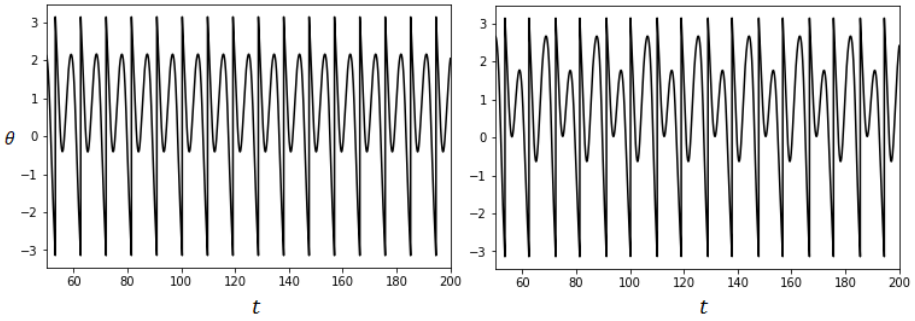

Figure 4: Trajectory of the pendulum with restricted values for θ at $f = 1.4$ (left) and $f = 1.45$ (right)

We can use a Poincaré section to simplify the presentation of the motion. The main idea is to cut or sample the 3 dimensional attractor (θ-ω-ϕ graph) periodically in ϕ. Here we plotted the values (θ_n, ω_n) in the θ-ω plane when $\phi = 2\pi n$, where n is an integer, at times in phase with the driving force. In our program, n ranges from 0 to 500, but we have waited for the first 20 cycles (the transient response) to die out. Then, we adjusted the value of θ after each iteration to keep it always between $-\pi$ and π for plotting purposes (Giordano, 2012, pp.48-71). Some specific results are shown below.

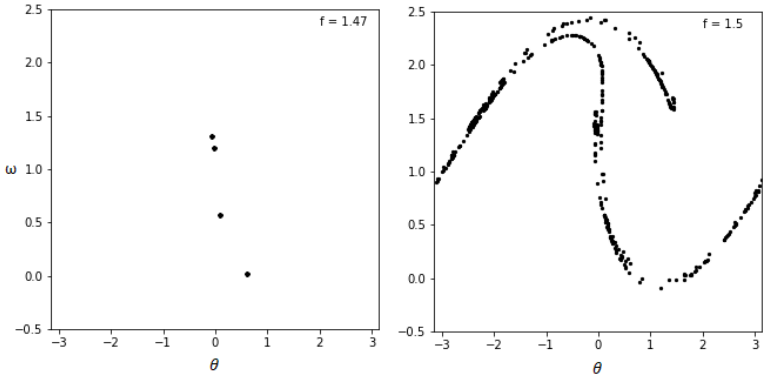

Figure 5: The Poincaré graph for two different values of f, 1.47 and 1.5, respectively

The Poincaré maps seen in Figure 5 corroborate the behaviour of the pendulum explained above concerning the phase space. As before, we kept all the parameters fixed except f. For example, we can see that when $f = 1.47$ there are four points represented. This corresponds to second doubling periodic (or period-4) rotations as stated before. For $f = 1.4$, $f = 1.45$ and $f = 1.12$, we get one, two and three points respectively. The latter result confirms that the angular velocity is $\Omega/3$. In general, the Poincaré cut of periodic attractors is represented by one or several points. However, the Poincaré cut of chaotic motion is as seen in Figure 5 (right). This is a very complex representation. A magnification of one small section can dissolve the line into several lines and

more magnifications show more and more closed curves. In reality, this split is finite.

4.2.2 Sensitivity to initial conditions

Figure 6 represents the change in θ with time that results for a change of 0.0001 in the initial conditions. For $f = 1.4$ (graph on the right), $\Delta\theta$ decreases approximately exponentially. In contrast, for chaotic cases, such as f = 1.2 (graph on the left), it increases roughly exponentially with an irregular and unpredictable motion.

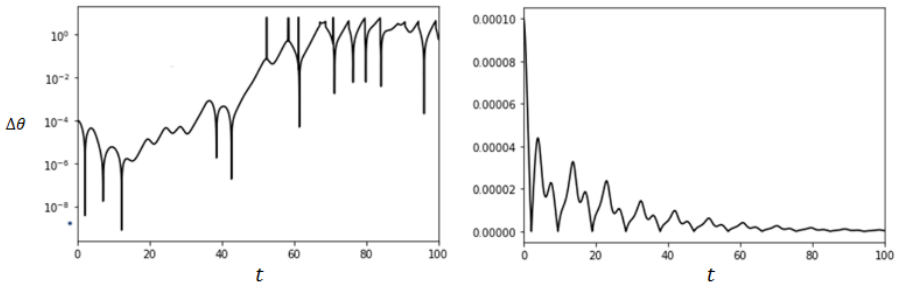

Figure 6: Change in θ when the initial conditions slightly vary.

The sharp dips in $\Delta\theta$ occur when the pendulum reaches a turning point and the two values of θ meet. Therefore, the plateau regions are more useful to investigate their trends. For the non-chaotic case of Figure 6 (right), we observed that $\Delta\theta$ rapidly becomes zero as the motion proceeds. Thus the trajectories converge, so we could predict its future motion without knowing its initial conditions. However, for the chaotic case shown at the left side of Figure 6, the two trajectories diverge from one to another until it has reached a value of order 2. We have used a logarithmic scale in chaotic cases because the increase of $\Delta\theta$ is very rapid. The graphs imply that $\Delta\theta \approx e^{\sigma t}$ where σ is a constant, which is called the Lyapunov exponent. In conclusion, for chaotic cases, the change of θ sharply increases, and the trajectories diverge from one another with time; however, for non-chaotic behaviours, the difference of the trajectories goes to zero as time increases.

4.2.3 Lyapunov exponents

The Lyapunov exponents quantitatively measure the sensitivity to initial conditions characteristic of chaotic behaviours. A program was created to calculate the average rate of divergence of a trajectory under a small perturbation, ϵ. The Lyapunov exponent in the ith-direction, σ_i, is given by $\lim_{t\to\infty}(1/t)ln[\epsilon(t)/\epsilon(t_0)]$. In practice, time went to 100, not ∞. The precision in the calculation of the exponents is not stationary, increases with time. The errors in the exponents were thus calculated by evaluating the standard deviation when the time series became stationary, i.e. when the statistical properties were constant.

The number of exponents agrees with the number of dimensions of the phase space. There are three Lyapunov exponents for the chaotic pendulum. The

exponent that corresponds to the ϕ degree of freedom (σ_3) is zero because it is parallel to the direction of the trajectory (Greiner, 2009, p.541). When the two other exponents are negative or zero, we find periodic states because the trajectories converge with time. If at least one of the exponents is positive, the system exhibits chaotic behaviour and the perturbed trajectory diverges exponentially from the original one. The first (principal) exponent determines the stability of the system. The consistency of the results can be checked by adding the exponents because the sum of all of them must be negative for dissipative systems and equal to the divergence of the velocity field (dissipation).

As an example, set the parameters at the values: $f = 1.12$, $\beta = 0.5$ and $\Omega = 2/3$. The Lyapunov exponents are given by -0.15 ± 0.01, -0.35 ± 0.01 and 0, the third exponent does not have any uncertainty, because there is no divergence or convergence in that direction and the average rate is 0 at any time. As none of the exponents is positive, the motion is shown to be periodic and indeed it describes non-chaotic behaviour. Moreover, the sum of the exponents is -0.5 ± 0.01 (within $-\beta$), the expected result. When $f = 1.2$, the Lyapunov exponents are 0.19, -0.69 and 0 with uncertainty 0.01. One of the exponents is positive, therefore the result exhibits chaos. As $\sigma_1 > 0$, the θ coordinate stretches by $e^{\sigma_1 t}$. However, the ω coordinate shrinks by $e^{\sigma_2 t}$ because $\sigma_2 < 0$. The first Lyapunov exponents and their errors are shown in Figure 7 as a function of f.

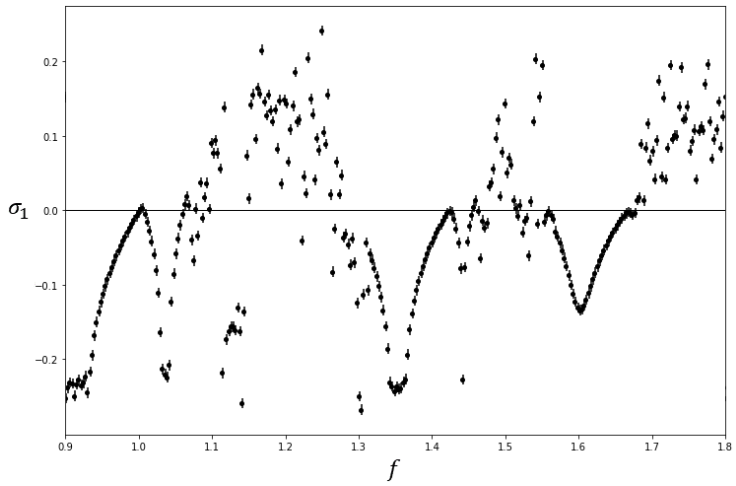

Figure 7: The principal Lyapunov exponents at different values of f

The Kaplan-Yorke relation calculates the Lyapunov dimension that, for the chaotic pendulum, is:

$$D_L = 1 + \frac{|\sigma_1|}{|\sigma_2|}. \tag{5}$$

The Lyapunov dimension highly depends on the damping term. When the pendulum is really damped, D_L is very small and; therefore, the attractor is compact and the points in the Poincaré graph are tightly packed (Baker and Gollub, 1996, p.125). For example, if the Lyapunov exponents are, as before,

0.19 ± 0.01, -0.69 ± 0.01 and 0, D_L is 1.28 ± 0.05. The uncertainty was calculated by propagating the errors of σ_1 and σ_2. This value of D_L is sensitive to β.

4.2.4 Bifurcation diagram

The bifurcation shows exactly how the transition from simple to chaotic behaviour takes place. The pendulum exhibits transitions to chaotic behaviour at different values of the driving force.

To make the calculation more efficient we have used a built-in function of Scipy that solves the differential equation quicker and with the required precision. We considered 350 values of f between $f = 0.9$ and $f = 1.8$. For each value of f, we obtained values of $\omega(t_n)$ where $t_n = t_0 + 2\pi n/\Omega$. The integer n goes from 0 to 30. When the system is periodic, we simply get one or several points. On the contrary, a chaotic motion will give many different points. To make the transient response decay away, the first 10 cycles were ignored.

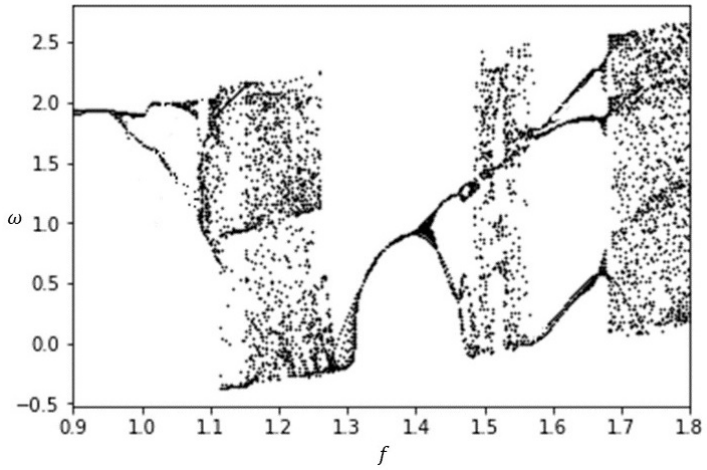

Figure 8: Bifurcation diagram. Graph of ω against f.

Figure 8 shows how the pendulum transits from period-1, period-2, period-4 to chaotic behaviours as the value of f changes from around 1.35 to 1.5. We also noticed that the spacing between period-doubling transitions shrinks as the order of the transition becomes bigger. There is symmetry between Figure 7 and 8. When $\sigma_1 > 0$, i.e. the behaviour of the pendulum is chaotic, there are many points represented in Figure 8. Periodic solutions occur when $\sigma_1 < 0$ and the bifurcation diagram at those values of f represents one or several points. The graphs are consistent with each other.

5 The Belousov–Zhabotinsky reaction

Now we will examine one of the most studied chemical systems according to Gyögyi and Field (1992) and a common example of chaos. The Belousov–Zhabotinsky reaction is a solution of citric acid in water with acidified bromate and ceric ions, characterised by a striking change of colours and the formation of compound rings.

This chemical system is not in thermodynamic equilibrium. The importance of the reaction comes precisely from the fact that it is far from equilibrium. Therefore, it can be explained by nonlinear dynamics and the theory of chaos. The reaction is also relevant because it can be empirically studied easily as it self-sustains for dozens of seconds.

5.1 Models

The system is very complex and consists of around 80 steps and 26 chemical species. We studied one model that considerably simplifies the problem and allows us to study the properties of chaos.

Some of the best-known models are the Brusselator, Oregonator and Gyögyi-Field models. The Brusselator model reduces the problem to two variables and, as the study of chaos requires at least three dynamical variables, it is not relevant for our purposes. The Oregonator model simplifies the reaction by rejecting those steps whose speed rate is much quicker than the others. Therefore, a speed rate limit is set. The results of this model are not shown because chaos is not seen; however, limit cycles appear. We instead studied a better approximation of the Belousov–Zhabotinsky reaction (The Gyögyi-field model). The reaction is now in a continuous stirred tank reactor (CSTR), in which the flow of products is continuous, and the composition is uniform in the reactor and at the exit. The steps are:

$$X + Y + H \rightarrow 2V \tag{6}$$

$$A + Y + 2H \rightarrow V + X \tag{7}$$

$$2X \rightarrow V \tag{8}$$

$$0.5X + A + H \rightarrow X + Z \tag{9}$$

$$X + Z \rightarrow 0.5X \tag{10}$$

$$V + Z \rightarrow Y \tag{11}$$

$$Z + M \rightarrow \tag{12}$$

where V is $BrCH(COOH)_2$, $H = H+$, $M = CH_2(COOH)_2$, $X = HBrO_2$, $Y = Br^-$ and $Z = Ce(IV)$. This gives the dimensionless equations of motion:

$$\frac{dx}{dt} = T_0[-k_1 H Y_0 x\hat{y} + k_2 A H^2 \frac{Y_0}{X_0}\hat{y} - 2k_3 X_0 x^2 + 0.5k_4 A^{0.5} H^{1.5} X_0^{-0.5}(C - Z_0 z)x^{0.5} - 0.5k_5 Z_0 xz - k_f x], \tag{13}$$

$$\frac{dz}{dt} = T_0[k_4 A^{0.5} H^{1.5} X^{0.5}(\frac{C}{Z_0} - z)x^{0.5} - k_5 X_0 xz - \alpha k_6 V_0 zv - \beta k_7 M z - k_f z], \tag{14}$$

$$\frac{dv}{dt} = T_0[2k_1 H X_0 \frac{Y_0}{V_0} x\hat{y} + k_2 A H^2 \frac{Y_0}{V_0}\hat{y} + k_3 \frac{X_0^2}{V_0} x^2 - \alpha k_6 Z_0 zv - k_f v]. \tag{15}$$

where $x = X/X_0$, $z = Z/Z_0$ and $v = V/V_0$. The parameters are described in the paper of Gyögyi and Field (1992). k_f is the inverse residence time of the reactor (amount of time the fluid could spend inside the reactor).

5.2 Simulations and results

The parameters at low CSTR flow are specified by Györgyi and Field (1992, pp.808-809) and the initial conditions were chosen to be $x = 0.0468627$, $z = 0.89870$ and $v = 0.84651$, points contained in the Poincaré plane. The step size used in the RK4 method was taken to be 1×10^{-5}, less precision does not give the right results and more precision is not required because the efficiency of the method considerably decreases and the results only improve by a tiny amount.

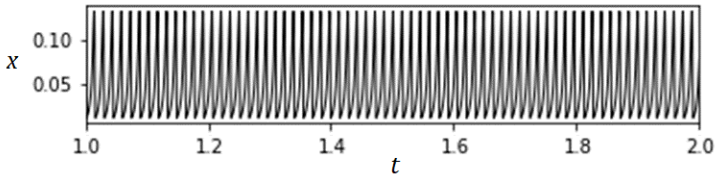

Figure 9: Variation of x with time when $k_f = 0.0003$.

The behaviour of the system when $k_f = 0.0003$, Figure 9, is periodic with period-1 cycles. We plotted the points from time 1 to make sure the transient response died out. Notice that this is not the representation of the real concentration of $HBrO_2$ with time.

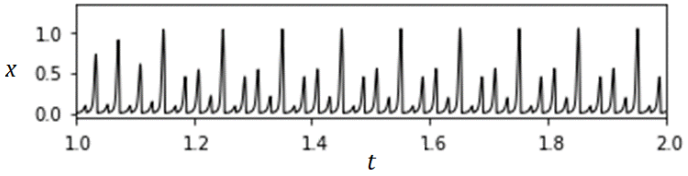

Figure 10: Variation of the x with time when $k_f = 0.00039$.

Figure 10 shows the evolution of the dimensionless concentration of $HBrO_2$ with time for $k_f = 3.9 \times 10^{-4}$. This graph represents period-5 oscillations. For example, when $k_f = 3.2 \times 10^{-4}$, it appears period-2 oscillations. At $f = 3.7 \times 10^{-4}$, period-3. Figure 11 shows the evolution of x with time when $k_f = 3.5 \times 10^{-4}$, the concentrations vary irregularly with time and the Lyapunov exponents give one positive and two negative exponents. The reaction exhibits the main properties of chaos for this value of k_f. The transitions from periodic to chaotic behaviours are shown in the bifurcation diagram of Figure 12.

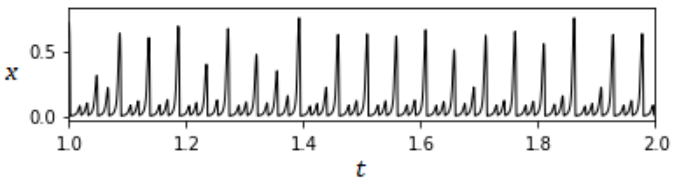

Figure 11: Variation of x with time for $k_f = 0.00035$.

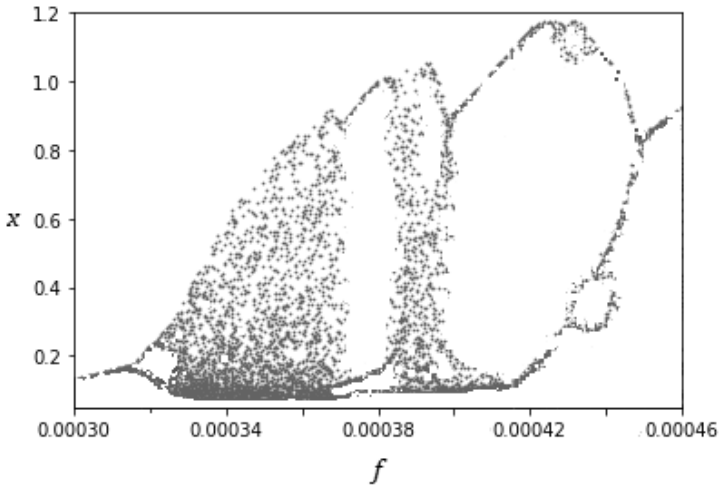

Figure 12: Bifurcation diagram at low CSTR flow.

Figure 12 corroborates the results stated above for low CSTR flow and we can clearly distinguish between chaotic and periodic solutions. Figure 13 shows the three dimensional attractor of the logarithms of the dimensionless concentrations when $k_f = 3.9 \times 10^{-4}$.

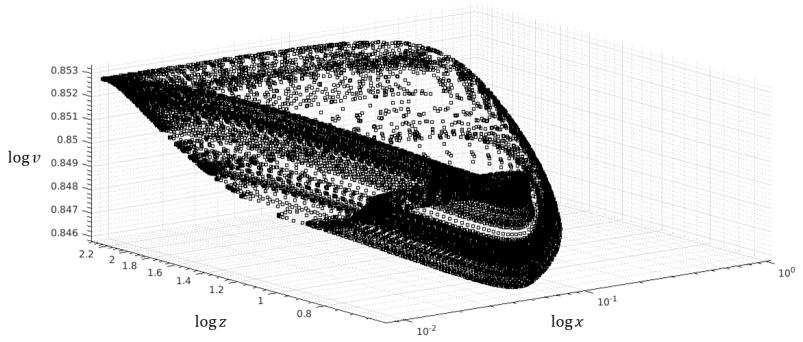

Figure 13: Attractor of the logarithms of the concentrations when $k_f = 0.00039$

6 Conclusions

The fourth-order Runge-Kutta method was used throughout the work and ensured good results because it was sufficiently accurate for our purposes. However, this method was very time-consuming when plotting the bifurcation diagram because we needed to implement the calculation for each value of f. The Lyapunov exponents were precisely calculated for the chaotic pendulum and the BZ reaction. These values corroborated the transitions from chaotic to periodic behaviours. All the results shown in the report were consistent with each other and were thoroughly evaluated with enough precision. We have successfully shown the irregularity and the unpredictability of both systems. These

two characteristics would imply the apparent randomness of the behaviour of them. Finally, given the strong similarities between the studied properties of the systems and the chaotic ones, the presence of chaos can be strongly claimed.

References

Acheson, D. (1997). From calculus to chaos: An introduction to dynamics. Oxford University Press on Demand.

Baker, G. L., Gollub, J. P. (1996). Chaotic dynamics: an introduction. Cambridge university press.

Belousov, B. P. (1959). Periodically acting reaction and its mechanism, 147, 145.

Chaitin, G.J. (2004), Meta math!. The quest for Omega. Retrieved from arXiv:math/0404335v7[math.HO]. doi. 10.5860/choice.43-4073

Giordano, N. J. (2012). Computational physics. Pearson Education India.

Greiner, W. (2009). Classical Mechanics: systems of particles and Hamiltonian dynamics. Springer Science Business Media.

Györgyi, L., Field, R. J. (1992). A three-variable model of deterministic chaos in the Belousov–Zhabotinsky reaction. Nature, 355(6363), 808-810.

Jones, E., Oliphant, T., Peterson, P. (2001). SciPy: Open source scientific tools for Python.

Lorenz, E. N. (1963). Deterministic nonperiodic flow. Journal of the atmospheric sciences, 20(2), 130-141..

Lorenz, E. (1972). Predictability: does the flap of a butterfly's wing in Brazil set off a tornado in Texas? (p. 181). na.

Van Rossum, G., Drake Jr, F. L. (1995). Python tutorial (Vol. 620). Amsterdam: Centrum voor Wiskunde en Informatica.

Zhabotinsky, A. M. (1964). Periodical oxidation of malonic acid in solution (a study of the Belousov reaction kinetics). Biofizika, 9, 306-311.

Appendix 1

This appendix evaluates the impact of COVID19 on the work completed and report.

Time lost travelling home: One of us travelled home and had problems (still unsolved) with their personal belongings.

Lack of access to computers and the internet: We worked on the project with the computers provided by the university. Our laptops are limited. We were not able to open the file we shared with our personal laptops. Fortunately, one of us had a copy of most of the work done.

Limitation in the outcome: We had some problems with communication and technology but the results presented and the quality of the report have not been very affected.